Domain Decomposition For Some Transmission Problems in Flow in Porous Media

Clarisse Alboin Jérôme Jaffré Jean E. Roberts
Xuewen Wang Christophe Serres

Abstract

A variety of models is considered: one-phase flow in a porous medium, two-phase flow in a porous medium with two rock types, one-phase flow in a porous medium with fractures. For each of these models the domain of calculation is divided into subdomains corresponding to the physics of the problem. Then it is shown how to rewrite the problems as interface problems in order to use nonoverlapping domain decomposition.

KEYWORDS: porous media flow, domain decomposition

1 Introduction

Domain decomposition methods have been studied for the most part as algebraic tools for solving problems on parallel machines: see [10] for a review of these methods. However in many models of flow in porous media arising from environmental problems in the subsurface as well as from reservoir simulation, the domain of calculation is naturally divided into subdomains corresponding to the physics of the problem. Therefore it is reasonable to construct nonoverlapping domain decomposition methods which can take into account the coupling of the physical phenomena taking place in the subdomains. In these methods one rewrites the global problem as a problem with unknowns on the subdomain interfaces.

After presenting in Section 2 the method for a simple case, namely one-phase flow, we show in Sections 3 and 4 how it applies to more complex problems: two-phase flow in a porous medium with two rock types and one-phase flow in a porous medium with fractures.

2 Single phase Darcy flow

We consider first the simple case of an incompressible single phase flow in a porous medium. The flow is governed by the following equations,

$$\begin{array}{rcll} \operatorname{div} \vec{\varphi} & = & 0, & \text{in } \Omega \\ \vec{\varphi} & = & -K \vec{\nabla} p, & \text{in } \Omega \end{array} \tag{2.1}$$

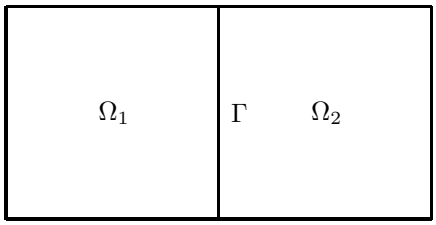

Figure 2.1: The domain Ω divided into two subdomains Ω_1 and Ω_2.

where Ω is a polygonal domain. The unknowns $\vec{\varphi}$ and p are the Darcy velocity and the fluid pressure and the coefficient K is the absolute permeability which may depend on $x \in \Omega$. To equations (2.1) we add the boundary conditions

$$p = p_d \text{ on } \partial\Omega_D, \quad \vec{\varphi} \cdot \vec{n} = q_d \text{ on } \partial\Omega_N, \tag{2.2}$$

where $\vec{n}$ denotes the outward normal to Ω. $\partial\Omega_D$ is the part of the boundary of Ω supporting Dirichlet boundary conditions and $\partial\Omega_N$ the part supporting Neumann boundary conditions, with $\partial\Omega = \partial\Omega_D \cup \partial\Omega_N$.

Now we divide the domain Ω into two polygonal subdomains Ω_1 and Ω_2 and we denote by Γ the interface between the subdomains: $\Gamma = \overline{\Omega}_1 \cap \overline{\Omega}_2$ (see Fig. 2.1). If we denote by $(\vec{\varphi}_i, p_i), i = 1, 2$, the restriction of the solution of the system of equations (2.1),(2.2) to the subdomain Ω_i, then we have

$$\begin{array}{rcll} \operatorname{div} \vec{\varphi}_i & = & 0 & \text{in } \Omega_i, \\ \vec{\varphi}_i & = & -K_i \vec{\nabla} p_i & \text{in } \Omega_i, \\ p_i & = & p_d & \text{on } \partial\Omega_i \cap \partial\Omega_D, \\ \vec{\varphi} \cdot \vec{n_i} & = & q_d & \text{on } \partial\Omega_i \cap \partial\Omega_N, \end{array} \tag{2.3}$$

with the transmission conditions

$$p_1 = p_2, \quad \vec{\varphi}_1 \cdot \vec{n}_1 = \vec{\varphi}_2 \cdot \vec{n}_2 \text{ on } \Gamma. \tag{2.4}$$

Here $\vec{n}_i$ is the outward normal to Ω_i. These conditions express continuity of the pressure and mass conservation.

Let us now discretize the subdomains Ω_i with a mesh $\mathcal{T}_i$ of triangles or parallelograms. To simplify we will assume that the two subdomain meshes are conforming in the sense that their union forms a regular discretization of the whole domain Ω. We denote by $\mathcal{E}_i$ the set of edges associated to $\mathcal{T}_i$.

To approximate the problem we use the Raviart-Thomas mixed finite elements of lowest order

[9, 1]. For this purpose we introduce the approximation spaces

$$\begin{aligned}
&\vec{X}_i(g) = \{\vec{v} \in \vec{RT}_0(\Omega_i) \mid \vec{v}\cdot\vec{n}_i = g \text{ on } \partial\Omega_i \cap \partial\Omega_N\},\\
&M_i = \{q \in L^2(\Omega_i) \mid q_{|C} \in P_0(C), C \in \mathcal{T}_i\},\\
&N = \prod_{E\in\Gamma} P_0(E).
\end{aligned}$$

Here $\vec{RT}_0(\Omega_i)$ denotes the Raviart-Thomas space of lowest order [8]; functions in this space are uniquely defined by their flux through the edges of $\mathcal{E}_i$. The Darcy velocity $\vec{\varphi}_i$ is calculated in this space. P_0 denotes the space of constants and M_i and N are spaces of piecewise constant functions defined on Ω_i and on Γ respectively. The pressure p_i inside Ω_i is approximated in M_i and the pressure on Γ denoted by λ is approximated in N. We will use the same notation for the approximating functions as for the solution of the continuous problem and we assume now that the boundary data functions p_d and q_d are constant on each interval of the discretized boundary $\partial\Omega$.

To solve the problem by nonoverlaping domain decomposition techniques we follow ideas from [5] to reduce the problem in Ω to an interface problem on Γ. We introduce Dirichlet-to-Neumann operators $\mathcal{S}_i$ associated to each subdomain Ω_i as follows. Given λ_i in N we solve the problem

$$\begin{aligned}
&\text{Find } \vec{\varphi}_i \in \vec{X}_i(q_d),\ p_i \in M_i \text{ such that}\\
&\int_{\Omega_i} \mathrm{div}\vec{\varphi}_i = 0,\\
&\int_{\Omega_i} K^{-1}\vec{\varphi}_i\cdot\vec{v} - \int_{\Omega_i} p_i\,\mathrm{div}\vec{v} + \int_{\partial\Omega_i\cap\partial\Omega_D} p_d\,\vec{v}\cdot\vec{n}_i\\
&\qquad\qquad + \int_\Gamma \lambda_i\,\vec{v}\cdot\vec{n}_i = 0, \quad \forall\vec{v} \in \vec{X}_i(0).
\end{aligned} \tag{2.5}$$

Then we define $\mathcal{S}_i$ by

$$\mathcal{S}_i(\lambda_i) = \vec{\varphi}_i\cdot\vec{n}_i\,|_\Gamma\,. \tag{2.6}$$

Our problem can now be rewritten as the following interface problem

$$\begin{aligned}
&\text{Find } \lambda_i \in N, i = 1,2, \text{ such that}\\
&\lambda_1 = \lambda_2, \quad \mathcal{S}_1(\lambda_1) + \mathcal{S}_2(\lambda_2) = 0.
\end{aligned} \tag{2.7}$$

The first equality corresponds to pressure continuity while the second corresponds to mass conservation (see equations (2.4)). The Dirichlet-to-Neumann operators $\mathcal{S}_i$ are affine. Denote by $\overline{\mathcal{S}}_i$ the linear part of $\mathcal{S}_i$ and by $\widehat{\mathcal{S}}_i$ the constant part: $\mathcal{S}_i(\lambda_i) = \overline{\mathcal{S}}_i(\lambda_i) + \widehat{\mathcal{S}}_i$. With $\lambda = \lambda_1 = \lambda_2$, the domain decomposition method is reduced to the linear problem

$$\begin{aligned}
&\text{Find } \lambda \in N \text{ such that}\\
&(\mathcal{S}_1 + \mathcal{S}_2)\lambda = F
\end{aligned} \tag{2.8}$$

where $F = \widehat{\mathcal{S}}_1 + \widehat{\mathcal{S}}_2$. One can now apply a conjugate gradient method to calculate λ. Preconditionners have been studied. For instance a Neumann-Neumann preconditionner has been presented and analyzed in [6]. For the case of a decomposition with many subdomains where some do not touch the boundary of Ω, the balancing domain preconditionner is robust with respect to strong variations of the permeability K [7, 3].

In the following sections we show how these domain decomposition techniques apply to a variety of situations.

3 Two-phase incompressible flow with two rock types

3.1 Formulation of the problem

We consider two-phase flow and we assume that the domain Ω is divided into two subdomains Ω_i, each subdomain corresponding to a rock type. This means that not only are the porosity and the absolute permeability different in Ω_1 and in Ω_2 but the relative permeability and capillary pressure curves are also.

Two-phase flow is formulated in terms of a saturation equation and a pressure equation using the global pressure [2]. We assume the flow to be incompressible and we neglect gravity.

The saturation equation expresses volume conservation for the wetting phase (which is equivalent to mass conservation since the flow is assumed to be incompressible), so inside each subdomain Ω_i we have:

$$\begin{aligned} &\Phi_i \frac{\partial S_i}{\partial t} + \operatorname{div} \vec{\varphi}_{wi} = 0, \\ &\vec{\varphi}_{wi} = \vec{r}_i + \vec{f}_i, \quad \vec{r}_i = -K_i a_i(S_i) \vec{\nabla} S_i, \quad \vec{f}_i = K_i b_i(S_i) \vec{\varphi}_i, \end{aligned} \tag{3.1}$$

where $S_i = S_{wi}$ is the saturation of the wetting phase ($0 < S_i < 1$). Here Φ_i and K_i denote the porosity and the absolute permeability, and $\vec{\varphi}_i$ is the total Darcy velocity, the sum of the Darcy velocities of the wetting and the nonwetting phases:

$$\vec{\varphi}_i = \vec{\varphi}_{wi} + \vec{\varphi}_{nwi}.$$

The coefficients a_i and b_i depend on the mobilities k_{wi} and k_{nwi} and the capillary pressure p_{ci} which are functions of the saturation:

$$a_i = \frac{k_{wi}\, k_{nwi}}{k_{wi} + k_{nwi}} \frac{dp_{ci}}{dS}, \quad b_i = \frac{k_{wi}}{k_{wi} + k_{nwi}}.$$

The capillary pressure is $p_{ci} = p_{nwi} - p_{wi}$ where p_{nwi} and p_{wi} denote the pressures in the nonwetting and wetting phases.

Plugging the first equation of (3.1) into the second, one obtains for saturation equation a nonlinear parabolic equation of diffusion-advection type. The vector $\vec{r}_i$, the diffusive contribution to $\vec{\varphi}_{wi}$, is due to capillary effects and $\vec{f}_i$, the advective contribution to $\vec{\varphi}_{wi}$, depends on the

total Darcy velocity $\vec{\varphi}_i$ which is given by the pressure equation that we now describe.

The pressure equation expresses the conservation of the total volume of the two phases. Since the flow is assumed to be incompressible this takes the form

$$\begin{aligned} &\operatorname{div} \vec{\varphi}_i = 0, \\ &\vec{\varphi}_i = -K_i d_i(S_i) \vec{\nabla} p_i \end{aligned} \tag{3.2}$$

where the global pressure p_i is given by

$$p_i = \frac{1}{2}(p_{wi} + p_{nwi}) + \gamma_i(S). \tag{3.3}$$

The coefficients γ_i and d_i are functions of the saturation S:

$$\gamma_i = \int_0^S (b_i(S) - \frac{1}{2}) \frac{dp_{ci}}{dS}, \quad d_i = k_{wi} + k_{nwi}.$$

Continuity of the phase pressures p_{wi} and p_{nwi} implies that the capillary pressure p_{ci}, and consequently the saturation S_i, is continuous, and that the global pressure p_i is also continuous (see definition 3.3). Also, because of phase conservation, the normal components of the phase Darcy velocities $\vec{\varphi}_{wi}$ and $\vec{\varphi}_{nwi}$, and consequently the normal components of the total Darcy velocity $\vec{\varphi}_i$, are continuous across any hypersurface.

Now we come to the transmission condition across Γ and we assume here for sake of simplicity that the two capillary pressure curves have the same endpoints.

Across the interface Γ we still have phase conservation and continuity of the phase pressures. This latter condition implies that the capillary pressure is continuous since it is the difference of the phase pressures, and that the quantity $p - \gamma$ is continuous (see equation (3.3)). Thus for the pressure equation we have the following transmission conditions

$$p_1 - \gamma_1(S_1) = p_2 - \gamma_2(S_2), \quad \vec{\varphi}_1 \cdot \vec{n}_1 = \vec{\varphi}_2 \cdot \vec{n}_2. \tag{3.4}$$

This implies that in general the global pressure p is discontinuous across Γ. The second equation of (3.4) enforces conservation of the global mass of the two phases.

For the saturation equation the transmission conditions are

$$p_{c1}(S_1) = p_{c2}(S_2), \quad \vec{\varphi}_{w1} \cdot \vec{n}_1 = \vec{\varphi}_{w2} \cdot \vec{n}_2 \quad \text{on } \Gamma. \tag{3.5}$$

Thus the saturation is discontinuous in general; the second equation enforces conservation of the mass of the wetting phase. One should note that the first equation is a nonlinear transmission condition for the saturation.

3.2 The pressure equation

To equations (3.2) we add boundary conditions (2.2). Equation (3.4) shows that the situation differs now from that in Section 2 in that the pressure p is discontinuous across Γ with a given jump.

We discretize with the same ideas as in Section 2, and we introduce the Dirichlet-to-Neumann operator $\mathcal{S}_i$ which associates to $\lambda_i \in N$ the flow rate $\vec{\varphi}_i \cdot n_i$ where $\vec{\varphi}_i$ is the solution of

$$\begin{aligned}
&\text{Find } \vec{\varphi}_i \in \vec{X}_i(q_d),\ p_i \in M_i \text{ such that} \\
&\int_{\Omega_i} \mathrm{div}\vec{\varphi}_i = 0, \\
&\int_{\Omega_i} (K_i d_i(S_i))^{-1} \vec{\varphi}_i \cdot \vec{v} - \int_{\Omega_i} p_i \,\mathrm{div}\vec{v} + \int_{\partial\Omega_i \cap \Gamma_D} p_d \,\vec{v} \cdot \vec{n}_i \\
&\qquad\qquad + \int_{\Gamma} (\gamma_i(S_i) + \lambda_i)\, \vec{v} \cdot \vec{n}_i = 0, \quad \vec{v} \in \vec{X}_i(0).
\end{aligned} \tag{3.6}$$

With this definition of the Dirichlet-to-Neumann operators the problem reduces again to problems (2.7) and (2.8). In this case λ represents $p - \gamma(S)$.

3.3 The saturation equation

To equations (3.1) we add the boundary conditions

$$S = S_d \text{ on } \partial\Omega_{SD}, \quad \vec{\varphi}_w \cdot \vec{n} = q_{wd} \text{ on } \partial\Omega_{SN}. \tag{3.7}$$

Discretizing the saturation equation is more complex than discretizing the pressure equation. Indeed it is a nonlinear parabolic equation, often advection dominated, with a diffusion term which degenerates when the saturation is minimum or maximum. We propose the use of a semi-implicit Euler discretization in time [4]. When calculating the saturation at the $n+1$ time level the advection term is lagging in time at the n time level and calculated with upstream values of the saturation, while the diffusion term is calculated at the $n+1$ time level with the nonlinear coefficient a lagging also at the previous time level. Thus at each time step one has to solve only a linear system to calculate the saturation.

We assume that the data S_d and q_{wd} are constant on each interval of the boundary $\partial\,\Omega$ and the approximation spaces for S_i and $\vec{\varphi}_{wi}$ are the same as in the previous sections. Actually since the advective part of the flow $\vec{f}_i$ is calculated at the previous time level, the main flow unknowm is the diffusive part of the flow $\vec{r}_i$.

In order to simplify the presentation, we assume that the domain Ω is rectangular, discretized with rectangles with sides parallel to the x_1 and x_2 coordinates axes so we can use a cell-centered finite volume method. Also the interface Γ is supposed to be parallel to the x_2 axis as in Fig. 2.1. We denote by $\partial\,\Omega_{iB}, \partial\,\Omega_{iT}, \partial\,\Omega_{iL}$ and $\partial\,\Omega_{iR}$ the bottom, top, left and right parts of the boundary $\partial\,\Omega_i$.

With these assumptions the discretized saturation equation is:

$$
\begin{aligned}
&\text{Find } \vec{r}_i \in \vec{X}_i(r_d^n),\ S_i \in M_i \text{ such that}\\
&\int_C \Phi_i \frac{S_i^{n+1}-S_i^n}{\Delta t} + \int_{\partial C} F_{wi}^{n*} = 0 \quad \forall C \in \mathcal{T}_i,\\
&F_{wi}^{n*} = \vec{r}_i^{\,n+1}\cdot \vec{n_C} + F_i^n,\\
&F_i^n = \vec{\varphi}_i^{\,n}\cdot \vec{n}_C\, b_i(S_{i-}^n),\\
&\vec{r}_i^{\,n+1}\cdot \vec{n}_E \mid_E = -\overline{K}_{iE}^H a(\overline{S}_{iE}^n)\frac{S_{iC_{E1}}^{n+1}-S_{iC_{E2}}^{n+1}}{h_E} \quad \forall E \in \mathcal{E}_i, E \not\subset \partial\Omega_{SN},\\
&S_{iC_{E1}}^{n+1} = S_d \text{ when } E \subset \partial\Omega_{SD} \cap (\partial\Omega_{iB} \cup \partial\Omega_{iL}),\\
&S_{iC_{E2}}^{n+1} = S_d \text{ when } E \subset \partial\Omega_{SD} \cap (\partial\Omega_{iT} \cup \partial\Omega_{iR}),\\
&S_{iC_{E2}}^{n+1} = \lambda_1 \quad \text{when } E \subset \Gamma,\ i=1,\\
&S_{iC_{E1}}^{n+1} = \lambda_2 \quad \text{when } E \subset \Gamma,\ i=2,
\end{aligned}
\tag{3.8}
$$

with the transmission conditions

$$
p_{c1}(\lambda_1) = p_{c2}(\lambda_2), \quad F_{w1}^{n*} + F_{w2}^{n*} = 0 \text{ on } \Gamma. \tag{3.9}
$$

We used the following notation: $\vec{n}_C$ is the outward normal to ∂C, $\vec{n}_E$ is the normal to the edge E pointing in the positive x_1 direction if E is vertical or pointing in the positive x_2 direction if E is horizontal, S_{i-}^n is the saturation value which is upstream with respect to $\vec{\varphi}_i^{\,n}$, and $r_d^n = q_{wd}^n - F_i^n$. When E is an interior edge we denote by C_{E1} and C_{E2} the two cells adjacent to E, $\overline{K}_{iE}^H$ denotes the harmonic average of K in these two cells, $\overline{S}_{iE}^n$ denotes the standard average of $S_{iC_{E1}}^{n+1}$ and $S_{iC_{E2}}^{n+1}$, and h_E is equal to the space discretization step. When E is a boundary edge $\overline{K}_{iE}^H$ is just the value of K in the neighbouring edge and h_E is equal to half the space discretization step.

To rewrite problem (3.8),(3.9) as an interface problem we proceed as before and we introduce for each subdomain Ω_i the linear Dirichlet-to-Neumann operator $\mathcal{S}_i$ defined as

$$
\mathcal{S}_i(\lambda_i) = (\vec{r}_i^{\,n+1}\cdot \vec{n}_i + F_i^n) \mid_\Gamma,
$$

where $\vec{r}_i^{\,n+1}$ is calculated by solving equations (3.8) inside each subdomain Ω_i with a given λ_i on Γ.

Our problem can now be rewritten as the following interface problem

$$
\begin{aligned}
&\text{Find } \lambda_i \in N, i=1,2, \text{ such that}\\
&p_{c1}(\lambda_1) = p_{c2}(\lambda_2), \quad \mathcal{S}_1(\lambda_1) + \mathcal{S}_2(\lambda_2) = 0.
\end{aligned}
\tag{3.10}
$$

One observes that the first equation is nonlinear and that the second equation implies that $\vec{r}\cdot n$ is discontinuous across Γ. One way to solve problem (3.10) is to use incomplete Newton iterations

with a preconditionned GMRES.

Remark: it is possible to make the diffusion term fully implicit. This would lead to use a nonlinear Dirichlet-to-Neumann operator.

3.4 A numerical example

As an example we consider the displacement of a nonwetting fluid by a wetting fluid with a mobility 10 times larger. The domain of calculation has two regions with different rock types, that on the left having an absolute permeability 5 times larger than that on the right. The injection is parallel to the interface Γ between the two rock types (see Fig. 3.1).

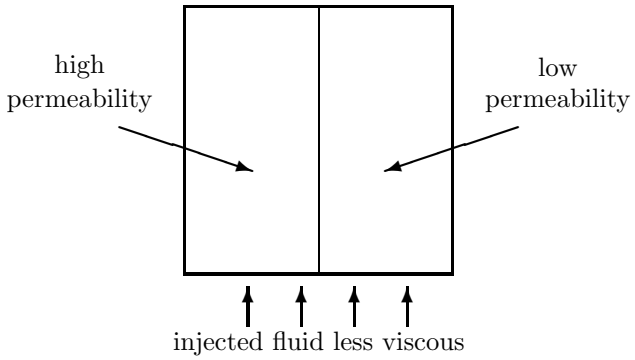

Figure 3.1: An example of a displacement in a medium with two rock types.

The capillary functions are given by the standard formula

$$p_c(S) = J(S)\sqrt{\frac{\Phi}{K}}$$

and are shown in Fig. 3.2. Since K is larger in Ω_1 than in Ω_2, the capillary pressure is smaller in Ω_1 than in Ω_2, so at the interface we can expect a discontinuous saturation smaller in Ω_1. Figure 3.3 shows numerical results at a certain time. The picture on the right shows the total Darcy velocity field $\vec{\varphi}$ at a certain time. Since the injection rate is constant along the bottom boundary and the permeability is low on the right the Darcy velocity in Ω_2 turns to the left in the vicinity of the injection boundary. The picture on the left shows the saturation of the injected fluid at the same time. One can observe the discontinuity at the interface. Note that along this interface, where the saturation is not equal to zero, the saturation is smaller on the left than on the right because the capillary pressure curve is smaller on the left than on the right. However further

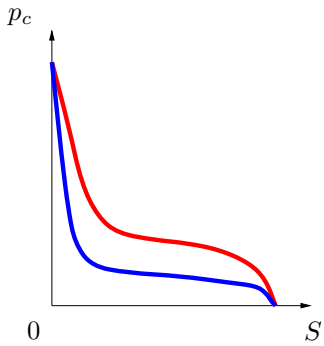

Figure 3.2: Capillary pressure curves, p_{c1} lower and p_{c2} upper.

away from this interface it is the opposite: the saturation, as the absolute permeability, is larger on the left than on the right.

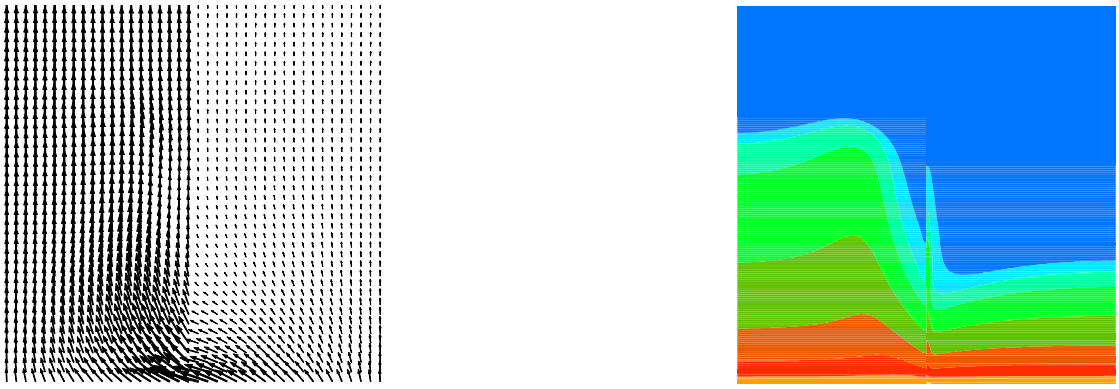

Figure 3.3: Calculated total Darcy velocity (left) and saturation (right).

4 Domain decomposition for flow in porous media with fractures

4.1 Formulation of the problem

In this section the domain Ω is divided into two subdomains $\Omega_i, i = 1, 2$, by a fracture Γ which is also a porous medium but with higher permeability. This fracture is assumed to have a width small compared to the size of the whole domain, so in the numerical model it is modelled as the interface Γ between the subdomains.

Here we are interested in understanding the interaction between the flow in the subdomains and the flow in the fracture. We assume that the flow in the subdomains as well as in the fracture is governed by Darcy's law, is incompressible and we neglect gravity.

Interaction between the fracture and the subdomains is assumed to satisfy mass conservation and pressure continuity. Thus we consider the following set of equations.

In the subdomains:

$$\begin{array}{rcll} \mathrm{div}(\vec{\varphi}_i) & = & 0 & \text{in } \Omega_i, \\ \vec{\varphi}_i & = & -K_i\vec{\nabla}p_i & \text{in } \Omega_i, \\ p_i & = & p_f & \text{on } \partial\Omega_i \cap \Gamma, \\ p_i & = & p_d & \text{on } \partial\Omega_i \cap \partial\Omega_D, \\ \vec{\varphi}_i \cdot \vec{n}_i & = & q_d & \text{on } \partial\Omega_i \cap \partial\Omega_N. \end{array} \tag{4.1}$$

In the fracture:

$$\begin{array}{rcll} \dfrac{\partial\,\varphi_f}{\partial\,x_f} & = & \vec{\varphi}_1 \cdot \vec{n}_1 + \vec{\varphi}_2 \cdot \vec{n}_2, & \text{on } \Gamma, \\ \varphi_f & = & -\sigma_f\, K_f \dfrac{\partial\, p_f}{\partial\, x_f} & \text{on } \Gamma, \\ p_f & = & p_{f,d} & \text{on } \partial\,\Gamma_D, \\ \varphi_f & = & q_{fd} & \text{on } \partial\,\Gamma_N. \end{array} \tag{4.2}$$

Here K_f, σ_f, p_f and φ_f denote the permeability, the width, the pressure and the flow rate in the fracture, and $\partial/\partial\,x_f$ denotes the derivative along the fracture.

At the extremities of the fracture there are Dirichlet (on $\partial\,\Gamma_D$) or Neumann (on $\partial\,\Gamma_N$) boundary conditions. If $\partial\,\Gamma_D$ touches $\partial\Omega_i \cap \partial\Omega_D$ then pressure continuity implies that the pressure data must satisfy $p_d = p_{fd}$.

The first equation (4.2) expresses mass conservation for the flow in the fracture. The right-hand side in this equation is the contribution of the subdomain flow to the fracture flow.

We proceed now as in Section 2, defining the same Dirichlet-to-Neumann operators (2.5),(2.6) and using the same notation. Moreover on Γ the pressure p_f is approximated in a space M_f of functions constant on each interval, while the flow rate φ_f is approximated in $X_f(q_{fd})$ a space of continuous piecewise linear functions which are equal to q_{fd} on $\partial\,\Gamma_N$.

This results in the following interface problem

$$\begin{array}{l} \text{Find } \varphi_f \in X_f(q_{fd}),\ p_f \in N \text{ such that} \\ \displaystyle\int_\Gamma \mathcal{S}_1(p_f) + \mathcal{S}_2(p_f) + \frac{\partial\,\varphi_f}{\partial\,x_f} = 0, \\ \displaystyle\int_\Gamma (\sigma_f\ K_f)^{-1}\varphi_f\, v - \int_\Gamma p_f \frac{\partial\, v}{\partial\, x_f} + (p_{fd}\, v)\mid_{\partial\,\Gamma_D} = 0 \quad \forall\, v \in X_f(q_0). \end{array}$$

Comparing with problem (2.8) we observe that the problem to be solved here is a global equation on the interface Γ.

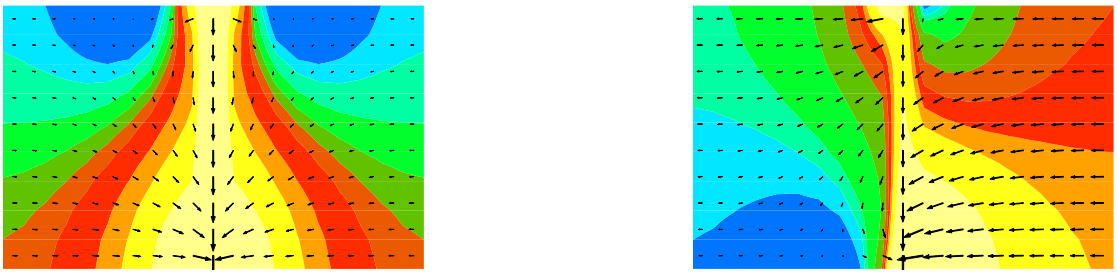

Figure 4.1: Calculated Darcy's velocity for a symmetric and a nonsymmetric flow pattern

4.2 A numerical experiment

To illustrate the model we consider an ideal dimensionless problem. The domain is an horizontal rectangular slice of porous medium, of dimensions 2×1, with a given pressure on the left and right boundaries and no flow conditions on the top and bottom boundaries. In the domain the permeability is equal to one. The domain is divided into two equally large sub-domains by a linear fracture parallel to the x_2 axis. In the fracture we chose $\sigma_f \ K_f = 2$. For example the fracture could be of width 0.1 and could have a permeability equal to 20.

Two cases are considered. A symmetric case where pressures on the left and on the right boundaries of the domain are equal. So the flow is driven only by the fracture and is symmetric. In the other case there is a pressure drop from the right boundary to the left one. Then the flow is a combination of the flow in the fracture and that going from left to right in the rest of the porous medium. Flow in the fracture is driven by a pressure drop of 10 between the two extremities of the fracture for the first case and a pressure drop of 5 for the second case.

Numerical results are shown on Fig. 4.1. Arrows represent the flow field with length proportional to the magnitude of the velocity. The gray scale represents the magnitude of the velocity with the lightest color corresponding to the largest velocity. We see that there is actual flow interaction between the fracture and the rest of the porous medium. In particular one can observe that some fluid is coming out of the fracture and then is coming back into it. In the nonsymmetric case we notice also that even though most of the flow is attracted into the fracture, there is still some flow on the left part of the domain pointing toward the left.

5 Conclusion

Studying a few examples of flow in porous media, we met a variety of transmission conditions which are nonstandard: discontinuity of the scalar variable (pressure or saturation), discontinuity of the flow rate variable (capillary flow), nonlinear transmission condition (saturation), nonlocal

transmission condition (porous medium with fractures). In spite of this variety of situations we showed that domain decomposition techniques based on Dirichlet-to-Neumann operators can be used to set these problems as interface problems to be solved using domain decomposition algorithms.

References

[1] Brezzi, F. and Fortin, M., *Mixed and Hybrid Finite Element Methods*. Springer Verlag, Berlin, 1991.

[2] Chavent, G. and Jaffré, J., *Mathematical Models and Finite Elements for Reservoir Simulation*, volume 17 of *Studies in Mathematics and its Applications*. North Holland, Amsterdam, Amsterdam, 1986.

[3] Cowsar, L. C., Mandel, J., and Wheeler, M. F., Balancing domain decomposition for mixed finite elements. *Math. of Comp.* **64** (1993), 989–1015.

[4] Douglas, Jr, J. and Dupont, T., Galerkin methods for parabolic equations. *SINUM* **7** (1970), 575–626.

[5] Glowinski, R. and Wheeler, M. F., Domain decomposition and mixed finite element methods for elliptic problems. In Glowinski, R. et al., editor, *Proceedings of the First Symposium on Domain Decomposition Methods for Partial Differential Equations*, SIAM, Philadelphia, 1987, 144–172.

[6] Le Tallec, P., De Roeck, Y.-H., and Vidrascu, M., Domain decomposition methods for large linearly elliptic three dimensional problems. *J. of Comp. and Applied Math.* **34** (1991).

[7] Mandel, J., Balancing domain decomposition. *Comm. in Numerical Methods in Engineering* **9** (1993), 233–241.

[8] Raviart, P.-A. and Thomas, J.-M., A mixed finite element method method for second order elliptic problems. In I. Galligani and E. Magenes, editors, *Mathematical Aspects of Finite Element Methods; Lecture Notes in Mathematics 606*, Springer, Berlin, 1977, 292–315.

[9] Roberts, J. E. and Thomas, J.-M., Mixed and hybrid methods. In P.G. Ciarlet and J.L. Lions, editors, *Handbook of Numerical Analysis Vol.II*, North Holland, Amsterdam, 1991, 523–639.

[10] Smith, B., Bjorstadt, P., and Gropp, W., *Domain Decomposition: Parallel Multilevel Methods for Elliptic Partial Differential Equations*. Cambridge University Press, 1996.

Clarisse Alboin, INRIA-Rocquencourt, BP 105, 78153 Le Chesnay Cedex, France, e-mail: Clarisse.Alboin@inria.fr

Jérôme Jaffré, INRIA-Rocquencourt, BP 105, 78153 Le Chesnay Cedex, France, e-mail: Jerome.Jaffre@inria.fr

Jean E. Roberts, INRIA-Rocquencourt, BP 105, 78153 Le Chesnay Cedex, France, e-mail: Jean.Roberts@inria.fr

Xuewen Wang, INRIA-Rocquencourt, BP 105, 78153 Le Chesnay Cedex, France, e-mail: Xuewen.Wang.Alboin@inria.fr

Christophe Serres, IPSN/DES/SESID, BP 6, 92265 Fontenay Aux Roses Cedex, France, e-mail: Christophe.Serres@ipsn.cea.fr